

AD-A114 065

AEROSPACE CORP EL SEGUNDO CA

F/8 20/8

A CLASSICAL TRAJECTORY CALCULATION OF THE O + H2 YIELDS OH + H --ETC(U)

APR 82 B R JOHNSON

F04701-81-C-0082

UNCLASSIFIED

TR-0082(2407-06)-1

SD-TR-82-20

NL

1 1/2
1 1/2



END

DATE

FILED

5-82

DTIC

REPORT SD-TR-82-20

AD A114065

A Classical Trajectory Calculation
of the $O + H_2 \rightarrow OH + H$ Cross Sections

B. R. JOHNSON
Chemistry and Physics Laboratory
Laboratory Operations
The Aerospace Corporation
El Segundo, Calif. 90245

12 April 1982

APPROVED FOR PUBLIC RELEASE:
DISTRIBUTION UNLIMITED

Prepared for
SPACE DIVISION
AIR FORCE SYSTEMS COMMAND
Los Angeles Air Force Station
P.O. Box 92960, Worldway Postal Center
Los Angeles, Calif. 90009

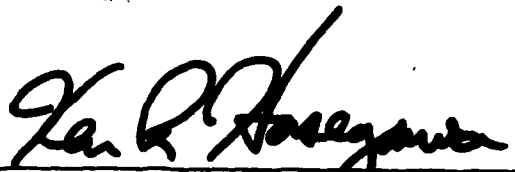



82 02 03 004

This report was submitted by The Aerospace Corporation, El Segundo, CA 90245, under Contract No. F04701-81-C-0082 with the Space Division, Deputy for Technology, P.O. Box 92960, Worldway Postal Center, Los Angeles, CA 90009. It was reviewed and approved for The Aerospace Corporation by S. Feuerstein, Director, Chemistry and Physics Laboratory. Lt Ken R. Hasegawa, SD/YLVM, was the project officer for the Mission-Oriented Investigation and Experimentation (MOIE) Program.

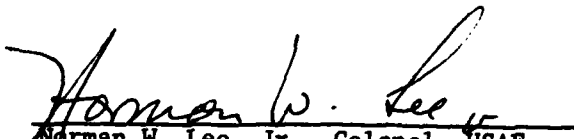
This report has been reviewed by the Public Affairs Office (PAS) and is releasable to the National Technical Information Service (NTIS). At NTIS, it will be available to the general public, including foreign nations.

This technical report has been reviewed and is approved for publication. Publication of this report does not constitute Air Force approval of the report's findings or conclusions. It is published only for the exchange and stimulation of ideas.


Ken R. Hasegawa, 2nd Lt, USAF
Project Officer


Florian P. Meinhardt, Lt Col, USAF
Director, Directorate of Advanced
Space Development

FOR THE COMMANDER


Norman W. Lee, Jr., Colonel, USAF
Deputy for Technology

UNCLASSIFIED

SECURITY CLASSIFICATION OF THIS PAGE (When Data Entered)

REPORT DOCUMENTATION PAGE		READ INSTRUCTIONS BEFORE COMPLETING FORM
1. REPORT NUMBER SD-TR-82-20	2. GOVT ACCESSION NO. AD A114065	3. RECIPIENT'S CATALOG NUMBER
4. TITLE (and Subtitle) A CLASSICAL TRAJECTORY CALCULATION OF THE $O + H_2 \rightarrow OH + H$ CROSS SECTIONS		5. TYPE OF REPORT & PERIOD COVERED
7. AUTHOR(s) Bernard R. Johnson		6. PERFORMING ORG. REPORT NUMBER TR-0082(2407-06)-1
9. PERFORMING ORGANIZATION NAME AND ADDRESS The Aerospace Corporation El Segundo, Calif. 90245		8. CONTRACT OR GRANT NUMBER(s) F04701-81-C-0082
11. CONTROLLING OFFICE NAME AND ADDRESS Space Division Air Force Systems Command Los Angeles, Calif. 90009		10. PROGRAM ELEMENT, PROJECT, TASK AREA & WORK UNIT NUMBERS
14. MONITORING AGENCY NAME & ADDRESS (if different from Controlling Office)		12. REPORT DATE 12 April 1982
		13. NUMBER OF PAGES 27
		15. SECURITY CLASS. (of this report) Unclassified
		15a. DECLASSIFICATION/DOWNGRADING SCHEDULE
16. DISTRIBUTION STATEMENT (of this Report) Approved for public release; distribution unlimited		
17. DISTRIBUTION STATEMENT (of the abstract entered in Block 20, if different from Report)		
18. SUPPLEMENTARY NOTES		
19. KEY WORDS (Continue on reverse side if necessary and identify by block number) Atomic Oxygen/Hydrogen Cross Sections Monte Carlo Classical Trajectory Calculation Reactive Scattering Rocket-Plume Signatures		
20. ABSTRACT (Continue on reverse side if necessary and identify by block number) State-to-state cross sections for the reaction $O + H_2(v, j) \rightarrow OH(v', j') + H$ are calculated by classical trajectory methods. The collision velocity and the initial vibration-rotation quantum numbers are chosen to be compatible with the values these parameters would have in a high-altitude missile plume-atmosphere interaction. The computed results are least squares fit to functional forms to provide simple working formulas for the cross sections. /		

DD FORM 1473
(FACSIMILE)

UNCLASSIFIED

SECURITY CLASSIFICATION OF THIS PAGE (When Data Entered)

CONTENTS

I.	INTRODUCTION.....	5
II.	POTENTIAL ENERGY SURFACE.....	7
III.	CALCULATIONS AND RESULTS.....	11
	A. Total Reactive Cross Sections.....	11
	B. Vibrational Distribution.....	12
	C. Rotational Distribution.....	19
REFERENCES	27

Accession For	
NTIS GRA&I	<input checked="" type="checkbox"/>
DTIC TAB	<input type="checkbox"/>
Unannounced	<input type="checkbox"/>
Justification	
By _____	
Distribution/	
Availability Codes	
Dist	Avail and/or Special

DTIC
COPY
INSPECTED
2

FIGURES

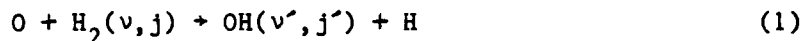
1.	The reactive cross section $\sigma_r(V; v, j)$	13
2.	The vibrational branching probability, $P(v' V, v, j)$, of the product $\text{OH}(v')$ molecule.....	16
3.	The cross section for the reaction $\text{O} + \text{H}(v, j) \rightarrow \text{OH}(v' = 1) + \text{H}$	18
4.	The thermally averaged cross sections for an assumed initial rotational temperature $T_R = 200^\circ\text{K}$ and various values of initial vibrational temperature T_V	20
5.	Product rotational distribution for the case $v = 1$, $j = 1$, $v' = 1$ and $E = 25 \text{ kcal/mol}$	23
6.	Product rotational distributions computed using the analytic fit Eqs. (14) - (21).....	24

TABLES

1.	Comparison of potential surfaces for $\text{O} + \text{H}_2$ in the saddle point region.....	8
2.	Least squares coefficients and threshold for calculating the total reactive cross sections $\sigma_r(V; v, j)$ by Eq. (5) in the text.....	14
3.	Least squares coefficients and threshold velocities for calculating the final vibrational distribution by Eq. (7) in the text.....	17

I. INTRODUCTION

The chemical reaction



and the subsequent radiative decay of the $v' = 1$ vibrational mode of the OH molecule at 2.8 μm , contribute to the infrared signature of certain high-altitude missile plumes. This reaction occurs when H_2 molecules present in the plume collide at high velocity with ambient atmospheric O atoms. Model calculations of the radiation generated by this process require as an essential input the state-to-state cross sections, $\sigma_r(v, j; v' = 1, j')$, of this reaction. The range of the initial vibration and rotation quantum numbers v and j , and the relative translational energy E of the reactants for which these cross sections are required, are determined by the velocity and temperature of the plume.

The velocity of the plume is the vector sum of the vehicle velocity and the rocket exhaust velocity. This will be a maximum in the retro-firing orientation where the two component velocities add. At high altitudes we can assume a vehicle velocity of about ~ 6 km/sec and a rocket exhaust velocity of about ~ 3 km/sec. In addition, the random thermal motion of the reactants will contribute ~ 1 km/sec, so the maximum relative collision velocity between the H_2 molecules in the plume and the atmospheric O atoms will be of the order of ~ 10 km/sec. This corresponds to ~ 22 kcal/mol of relative translational energy between the (O, H_2) reactants.

The temperature of the plume decreases rapidly due to expansion after leaving the rocket nozzle. Along a given streamline the collision frequency decreases and at some point is not sufficient to maintain thermal equilibrium between the vibrational, rotational and translational modes. The vibrational modes are the first to decouple and are said to freeze out at a vibrational temperature T_v . Further along the streamline and at a lower temperature T_R , the rotational modes freeze out. Typically, the rotational temperature will

be quite low. We have assumed that $T_R < 200^\circ\text{K}$. At this temperature only the $j = 0,1$ rotational states of H_2 will be significantly populated. The vibrational temperature T_V is higher than the rotational temperature, but is certainly much less than the temperature inside the rocket engine, which is about $\sim 3000^\circ\text{K}$. Even using this very crude upper limit, the conclusion is that only the $v = 0$ and $v = 1$ vibrational modes of H_2 will be sufficiently populated to contribute significantly to the reactive cross section.

We report here the results of a Monte Carlo classical trajectory study of the state-to-state cross sections for reaction (1). These cross sections are determined in the range of relative kinetic energy, from the lowest threshold of 4 kcal/mol to an upper value of 25 kcal/mol and for initial vibration-rotation quantum numbers in the range $v = 0,1$; $j = 0,1$. The potential surface used in these calculations is discussed in Section II. The calculational procedure and the cross section results are given in Section III.

II. POTENTIAL ENERGY SURFACE

The potential function used in this study is the same potential employed by Johnson and Winter (JW)¹ in a previous classical trajectory study of the (O, H_2) system. This function is a London-Eyring-Polanyi-Sato (LEPS) surface with a single Sato parameter adjusted by trial and error to yield a computed rate constant in agreement with experimental data around 320 K. Rate constants computed with this potential were in good agreement with the best experimental measurements over the temperature range 300 K to 1000 K. This potential was also used to calculate the rate constant for the reaction $O + H_2(v = 1) \rightarrow OH + H$, where the H_2 has a single quantum of vibrational energy.¹ Light² has since measured this rate at $T = 302$ K. The computed result is in reasonably good agreement with the experimental value.

Recently, two groups, Howard, McLean and Lester (HML)³, and Walsh, Danning, Raffanetti and Bobrowicz (WDRB)⁴, have published ab initio configuration interaction calculations of the potential surface for the $O(^3P) + H_2(^1\Sigma_g^+)$ reaction which can be compared to the JW LEPS surface. The saddle point properties of the three surfaces are compared in Table 1. We see that the JW potential and the WDRB potential both have the same barrier height of 12.5 kcal/mol, while the HML potential is 14.0 kcal/mol. Shinke and Lester have fit the HML surface to a 56-parameter function by least squares and used it in a classical trajectory study⁵ of the $O + H_2$ system. Their calculated rate constants $k(v)$ for the reaction $O + H_2(v) \rightarrow OH + H$ are less than the experimental values over the entire temperature range from 300 K to 1000 K for the case $v = 0$ and are also less than Light's experimental value for the case $v = 1$. This strongly indicates that the 14.0 kcal/mol barrier height of the HML potential is too high.

For noncollinear geometries the potential surface splits into two distinct surfaces of $^3A'$ and $^3A''$ symmetry. WDRB have calculated both these surfaces. In the saddle point region, the only different property of the $^3A'$ and $^3A''$ surfaces is the bending potential curve. The bending curve of the JW surface is approximately the average of these two curves⁴ and thus

Table 1. Comparison of potential surfaces for
 $O + H_2$ in the saddle point region.

	ΔE kcal/mol	r_{HH} Å	r_{OH} Å
Johnson, Winter LEPS	12.5	0.95	1.12
Howard, McLean and Lester, ab initio	13.95	0.95	1.15
Walch, Dunning, Raffenetti and Bobrowicz, ab initio	12.5	0.93	1.21

represents a very good single-surface compromise to using two surfaces for dynamical calculations.

Given these comparisons of the JW surface with the ab initio surfaces and the good agreement of the JW calculated rate constants with the experimental values, and taking account of the uncertainties in both the ab initio potentials and the measured rate constants, we believe that the simple JW LEPS potential is at least as good as the ab initio potentials and is a good approximate surface for use in the present classical trajectory calculations.

III. CALCULATIONS AND RESULTS

A. TOTAL REACTIVE CROSS SECTIONS

Muckermann's classical trajectory program, CLASTR,⁶ which is based on the analysis of Karplus, Porter and Sharma⁷, was used to calculate the cross sections. Essential inputs to the program, necessary to define the initial state of the reactants, are the separation of the reactants r_0 , the relative kinetic energy E , and the vibration-rotation quantum numbers v and j . Two other required input quantities are b_{\max} , the maximum value of the impact parameter, and N_{TOT} , the total number of trajectories to be calculated. The program computes N_{TOT} trajectories, selecting initial conditions by the quasi-classical Monte Carlo procedure;⁷ it classifies each trajectory as reactive or not reactive; and it calculates, by the histogram binning method, the vibration-rotation quantum numbers v' and j' of the product diatomic molecule. The output of the program is $N_r(E; v, j; v', j')$, which is the number of reactive trajectories out of the total number $N_{\text{TOT}}(E, v, j)$ that started in state v, j and ended in the product state v', j' .

A series of calculations on the (O, H_2) system were carried out using this program. The initial separation in all cases was $r_0 = 4 \text{ \AA}$, the kinetic energy was sampled in the range $4 < E < 25 \text{ kcal/mol}$, and the initial vibration-rotation quantum numbers were $v = 0, 1$ and $j = 0, 1$.

For maximum computational efficiency, b_{\max} should not be any greater than the maximum impact parameter for which a reaction occurs. This varies, depending on E , v and j . We were able to make use of our previous calculations on this system¹ to obtain reliable estimates of b_{\max} . For $v = 0$, b_{\max} was varied between 0.6 \AA and 1.4 \AA and for $v = 1$ it was varied between 1.2 \AA and 1.9 \AA depending on the energy E . N_{TOT} was also varied, depending on the values of E and v . For $v = 1$, $N_{\text{TOT}} = (400 - 1200)$ trajectories, and for $v = 0$, $N_{\text{TOT}} = (1200 - 2000)$ trajectories. In general the larger number of trajectories were used at low energies, where the reactive cross section is small, in order to maintain enough reactive trajectories to calculate with reasonable statistical accuracy the final vibration-rotation distribution.

The total reactive cross sections for a specific collision energy E and initial vibration-rotation state v, j is computed by the formula⁷

$$\sigma_r(E, v, j) = \pi b_{\max}^2 N_r(E, v, j) / N_{\text{TOT}}(E, v, j) \quad (2)$$

where

$$N_r(E, v, j) = \sum_{v'} \sum_{j'} N_r(E, v, j; v', j') \quad (3)$$

is the total number of reactive trajectories without regard to the final vibration-rotation state.

The relative kinetic energy in these calculations was specified in kcal/mol. It will be more convenient to give the results of our calculations in terms of relative velocity rather than energy. The relation between velocity V (in kilometers/sec) and energy E (in kcal/mol) for the (O, H_2) system is

$$V = 2.162 E^{1/2} \quad (4)$$

The cross sections computed using Eq. (2) are plotted versus velocity in Fig. 1. The solid lines are least squares fits of the computed points to the cubic polynomial function

$$\sigma_r(V, v, j) = [(a_3 V + a_2)V + a_1]V + a_0. \quad (5)$$

This fit is valid in the range of velocities $V_T(v, j) < V < 11 \text{ km/sec}$, where $V_T(v, j)$ is the threshold for the reaction. The coefficients and the thresholds are given in Table 2.

B. VIBRATIONAL DISTRIBUTION

The probability that a reactive trajectory will terminate in a particular vibrational state v' of the product OH molecule is given by

$$P(v' | V, j, v) = \sum_{j'} N_r(V, v, j; v', j') / N_r(V, v, j) \quad (6)$$

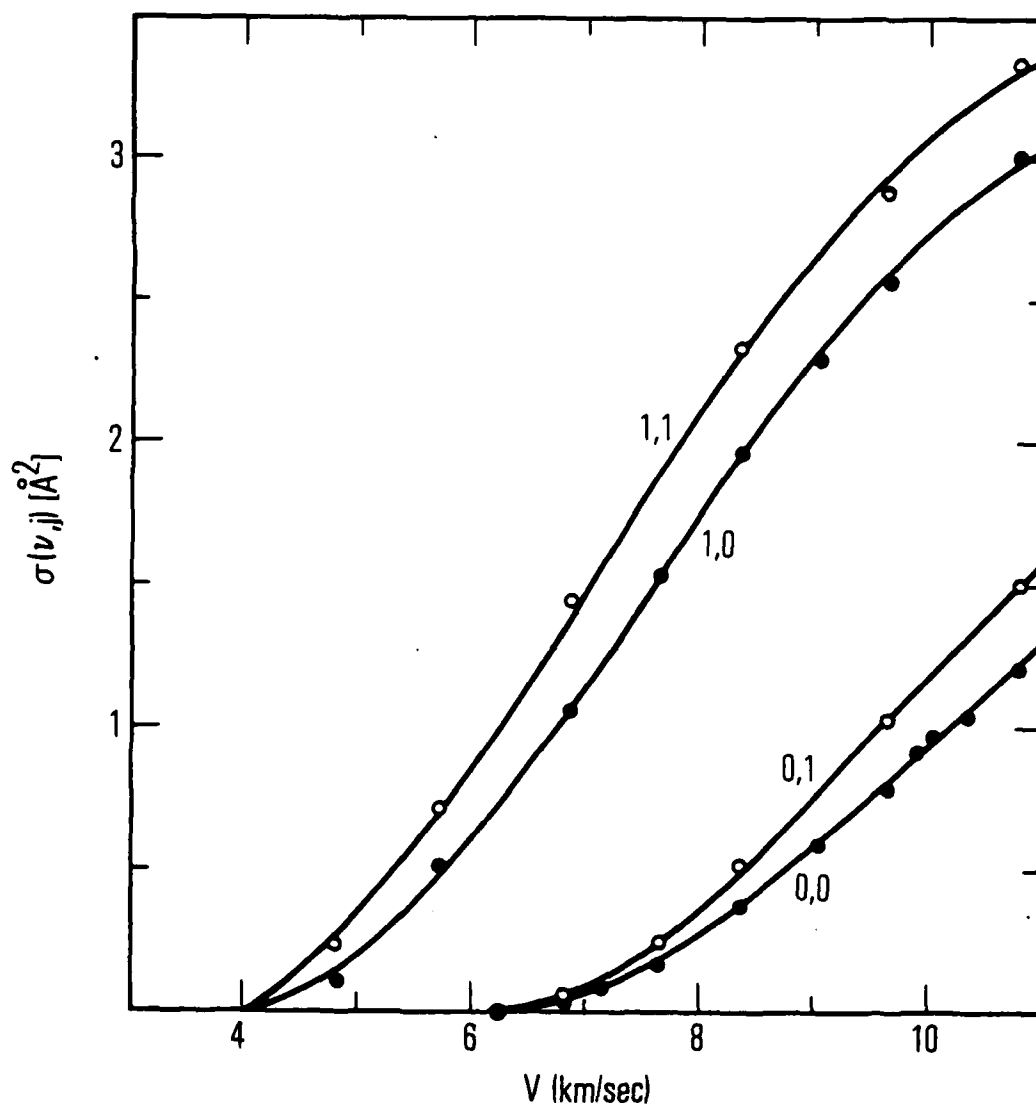


Figure 1. The reactive cross sections $\sigma(V; \nu, j)$. The labels are the initial quantum numbers ν, j . The dots are the computed values, the solid curves are the least squares fits using Eq. (5) and the coefficients in Table 2.

Table 2. Least squares coefficients and threshold velocities for calculating the total reactive cross sections $\sigma_r(V; v, j)^a$ by Eq. (5) in the text.

v	j	a_0	a_1	a_2	a_3	v_T^b
0	0	6.8009	-2.5892	0.30647	-0.010608	6.27
0	1	8.6803	-3.3532	0.40406	-0.014363	6.27
1	0	2.9638	-1.7619	0.30914	-0.013505	4.03
1	1	1.6626	-1.2653	0.2607	-0.011947	3.98

^aThe cross section units are \AA^2 .

^bVelocity units are kilometers/sec.

These probabilities are plotted versus the collision velocity in Fig. 2. The solid lines are (segmented) linear least squares fits where the discontinuous change in slopes occurs at the threshold for exciting the $v' = 1$ state in Fig. 2a and at the threshold for $v' = 2$ in Fig. 2b. Above the thresholds the probabilities are given by the linear fit

$$P(v'|V, v, j) = b_0 + b_1 V. \quad (7)$$

The coefficients and thresholds are given in Table 3.

The state-to-state reactive cross sections $\sigma_r(V, v, j; v')$ are obtained by multiplying the total cross sections by the conditional probability that if a reaction occurs it will terminate in the v' th state

$$\sigma_r(V, v, j; v') = P(v'|V, v, j) \sigma_r(V, v, j) \quad (8)$$

An analytic expression for this cross section is the product of the least squares formulas (5) and (7). It is

$$\sigma_r(V, v, j; v') = (b_0 + b_1 V) [(a_3 V + a_2) V + a_0] \quad (9)$$

which is valid for velocities in the range from the thresholds given in Table 3 to ~ 11 km/sec. For convenience we have calculated the cross sections for the case $v' = 1$ which are needed for plume signature studies and plotted them in Fig. 3. It is evident from this figure that the reactive cross section for producing $\text{OH}(v' = 1)$ is greatly enhanced by a quantum of vibrational energy in the H_2 reactant molecule. This will have a significant effect on the rate of production of $\text{OH}(v' = 1)$ only if the reactants initially have a significant $\text{H}_2(v' = 1)$ population, i.e., if the vibrational temperature of the H_2 is high enough.

The effect of the initial vibration and rotation temperatures of the reactants can be taken account of by defining a "distribution averaged" cross section.

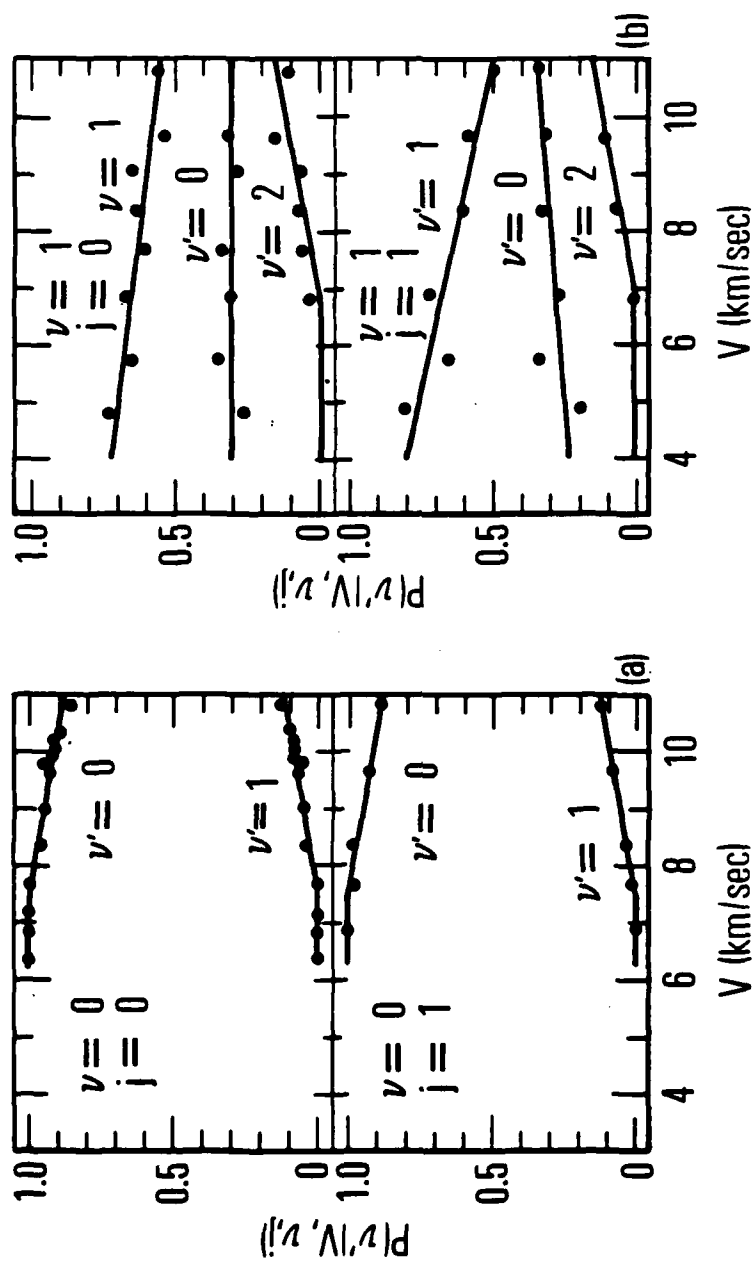


Figure 2. The vibrational branching probability, $P(v'|V, v, j)$, of the product $\text{OH}(v')$ molecule. The dots are the computed values, the solid lines are a least squares fit.

Table 3. Least squares coefficients and threshold velocities for calculating the final vibrational distribution by Eq. (7) in the text.

v	j	v'	b_0	b_1	v_T^a
0	0	0	1.242	-0.0323	7.5
0	0	1	-0.242	0.0323	7.5
0	1	0	1.256	-0.0346	7.4
0	1	1	-0.256	0.0346	7.4
1	0	0	0.310	0.0003	4.0
1	0	1	-0.827	-0.0252	4.0
1	0	2	-0.245	0.0361	6.8
1	1	0	0.117	0.0159	4.0
1	1	1	0.976	-0.0431	4.0
1	1	2	-0.237	0.0356	6.7

^aVelocity units are kilometers/sec.

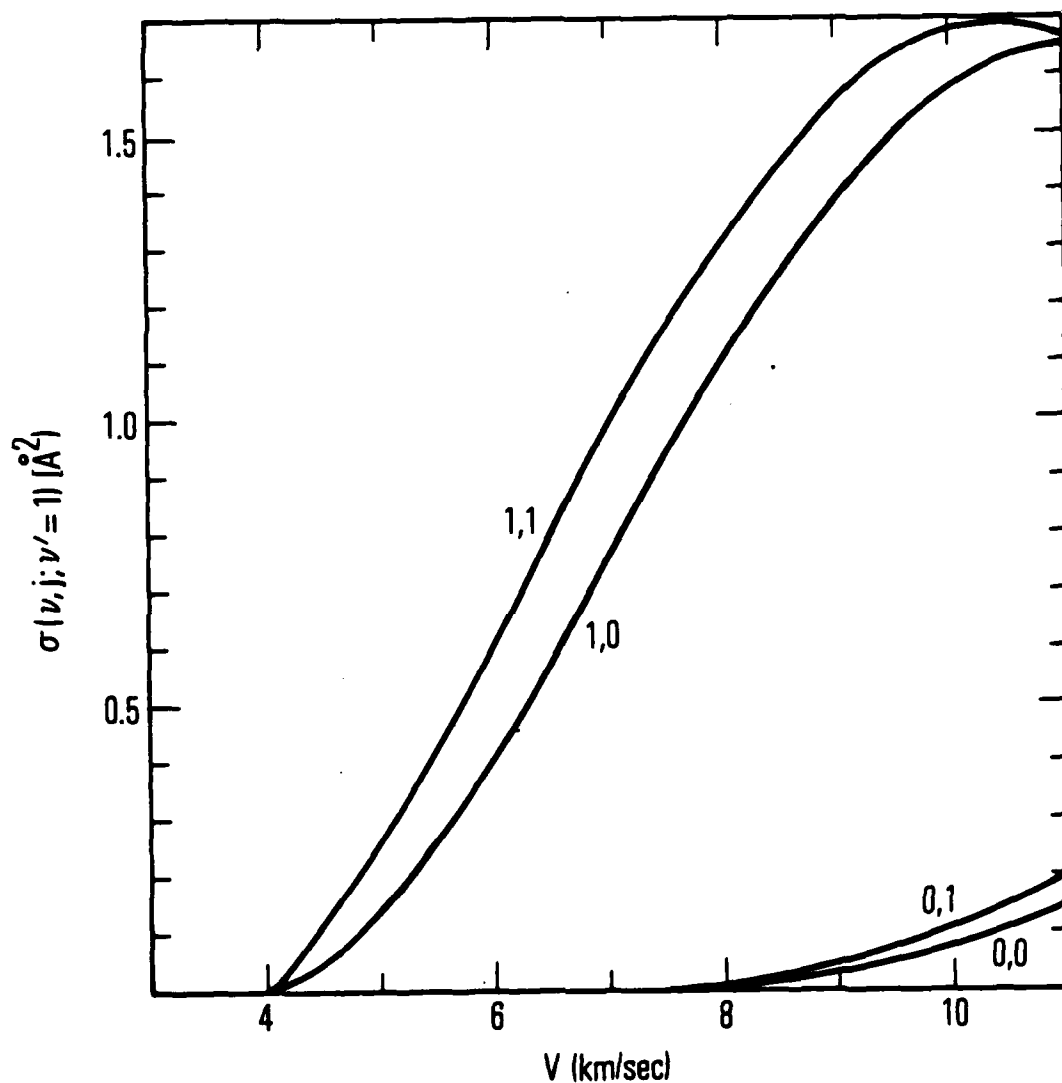


Figure 3. The cross section for the reaction $O + H(v, j) \rightarrow OH(v' = 1) + H$. The curves were calculated using Eq. (8) and the coefficients in Tables 2 and 3. The labels on the curves are v, j .

$$\sigma_r(v, T_V, T_R; v') = Q^{-1} \sum_v \sum_j g_j (2j + 1) \exp[-E_V(v)/kT_V - E_R(v, j)/kT_R] \sigma_r(v, v, j; v') \quad (10)$$

In this equation T_V and T_R are the vibration and rotation temperatures, k is Boltzmann's constant, g_j is the ortho-para-statistical weight factor ($g_j = 1$ for even j , $g_j = 3$ for odd j), $E_V(v)$ and $E_R(v, j)$ are the vibration and rotation energies of $H_2(v, j)$, and Q is the normalizing partition function obtained by evaluating the sum in Eq. (10) with the last cross section factor equal to unity. The vibration and rotation energies can be adequately approximated using the simple vibrating-rotor formulas⁸

$$E_V(v) = \omega_e(v + \frac{1}{2}) - \omega_e x_e(v + \frac{1}{2})^2 \quad (11)$$

and

$$E_R(v, j) = B_v j(j + 1); \quad B_v = B_e - \alpha(v + \frac{1}{2}) \quad (12)$$

where the symbols have their usual meaning.

We have used Eq. (10) to evaluate the "distribution-averaged" cross section curves for the production of $OH(v' = 1)$ for a fixed rotational temperature $T_R = 200^\circ K$ and three values of the vibrational temperature $T_V = 1000^\circ K$, $1500^\circ K$ and $2000^\circ K$. These are plotted versus velocity in Fig. 4. Below $1000^\circ K$ the contribution of $v = 1$ to the reaction rate is quite small, although for velocities less than the threshold of 7.4 km/sec it represents the only contribution. Above $1000^\circ K$ the $v = 1$ states of the reactant H_2 molecules significantly increase the cross sections.

These calculations were repeated for two other rotational temperatures, $T_R = 100^\circ K$ and $T_R = 300^\circ K$, with very little change from the $200^\circ K$ results shown in Fig. 4. This is to be expected since the state-to-state cross sections are not strongly dependent on the rotational states.

C. ROTATIONAL DISTRIBUTION

In a given final vibrational state v' , the probability distribution over the rotational states j' is given by

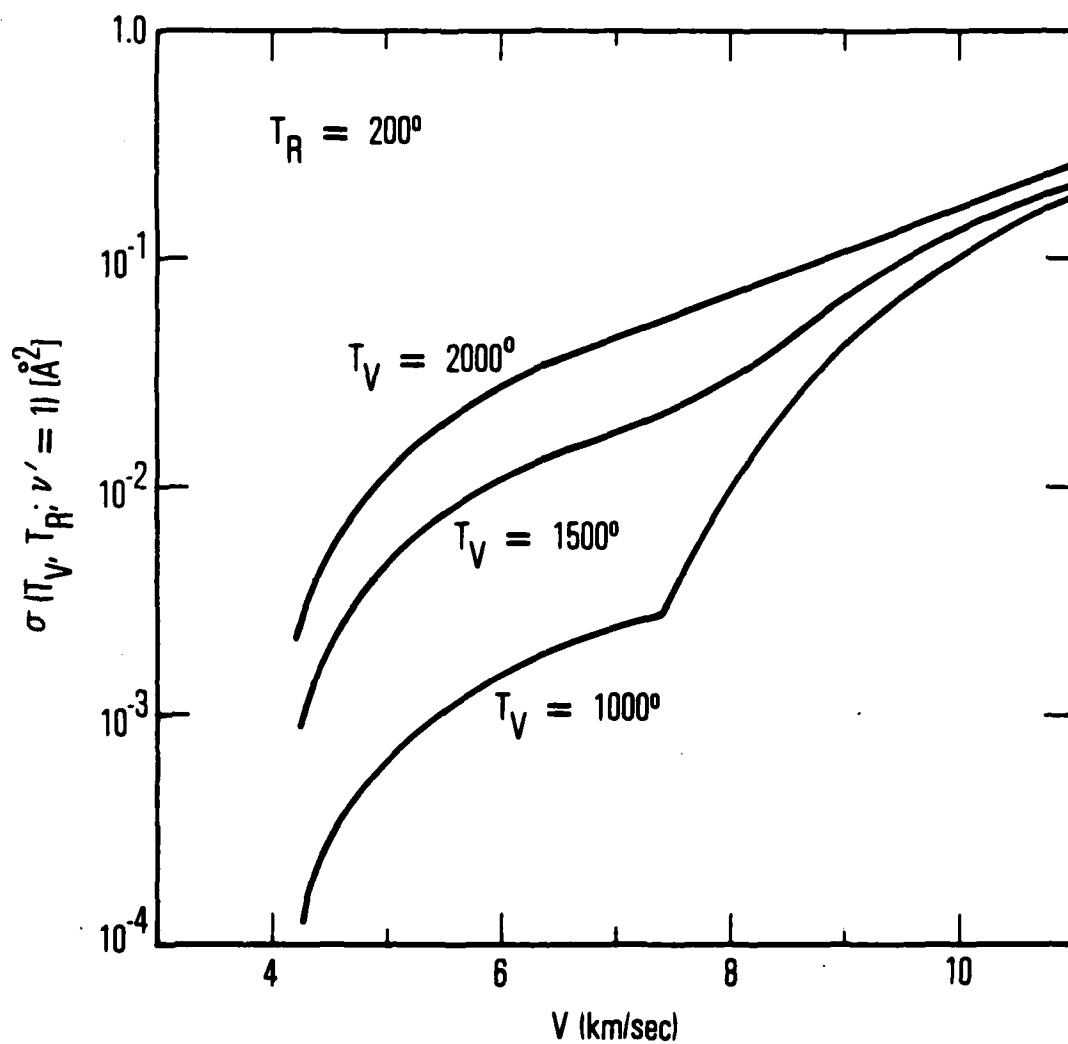


Figure 4. The thermally averaged cross sections for an assumed initial rotational temperature $T_R = 200^\circ\text{K}$ and various values of initial vibrational temperature T_V . These curves were computed using Eq. 10.

$$P(j'|v'; V, v, j) = N_r(V, v, j; v', j') / \sum_{j'} N_r(V, v, j; v', j') \quad (13)$$

These conditional probabilities were computed and then fit to the analytic function

$$P(j'|v'; V, v, j) = (2j' + 1)[U - j'(j' + 1)]^{1/2} \exp[-\theta j'(j' + 1)/U]/Q \quad (14)$$

This function has been used in previous work to represent rotational distributions⁹ and is derived by information theoretic methods.^{10,11} The normalization constant Q is determined by the condition

$$\sum_{j'=0}^{j_{\max}} P(j'|v'; V, v, j) = 1 \quad (15)$$

The quantity U is defined to be

$$U = [E + E_{v,j} - E_{v'} - \Delta]/B_{v'} \quad (16)$$

where E is the relative kinetic energy of the reactants, $E_{v,j}$ is the vibrational-rotational energy levels of H_2 , $E_{v'}$ is the vibrational energy levels of OH , $\Delta = 2.79$ kcal/mol is the endothermicity of the reaction measured with respect to the potential energy minima of the product and reactant channels, and $B_{v'}$ is the rotational constant of OH in the v' th vibrational level. Finally, θ is the rotational surprisal parameter which can be adjusted to obtain a fit to the trajectory-computed rotational distributions. The quantity j_{\max} in Eq. (15) is the maximum value of the rotational quantum number allowed by energy conservation. It is the integer part of the solution of the equation

$$j_{\max}(j_{\max} + 1) = U \quad (17)$$

The quantity U , defined by Eq. (16), depends on the quantum numbers v, j and v' . However, the dependence on j is weak and can be ignored. Also, for

the rocket plume signature calculations we only need to determine the rotational distributions associated with the $v' = 1$ vibrational mode. Therefore, we need only consider two functional forms for U , corresponding to $v = 0$ and $v = 1$. To sufficient accuracy they are

$$U_0 = (E - 12.5)/0.051 \quad (18)$$

and

$$U_1 = E/0.051 \quad (19)$$

where U and E are in units of kcal/mol.

These expressions are then substituted into Eqs. (14) and (15) to obtain the rotational distributions and j_{\max} . To obtain reasonable fits to the computed distributions it was found that the parameter θ was dependent only on v and that the data could be fit using

$$\theta = 1.0, (v = 0) \quad (20)$$

and

$$\theta = 0, (v = 1) \quad (21)$$

Calculation of the rotational distribution using Eq. (14) is easily implemented on a computer or even a programmable calculator.

Figure 5 shows a comparison of the actual trajectory-calculated rotational distribution, plotted as a histogram, and the fitted function which is shown as a continuous curve, for a typical case $v = 1$, $j = 1$, $v' = 1$ and $E = 25$ kcal/mol. Figure 6 shows how the rotational distributions vary as a function of the initial vibration state v and the relative kinetic energy of the reactants.

The final partitioning of the state-to-state reactive cross section into its constituent product rotational states can now be computed by multiplying

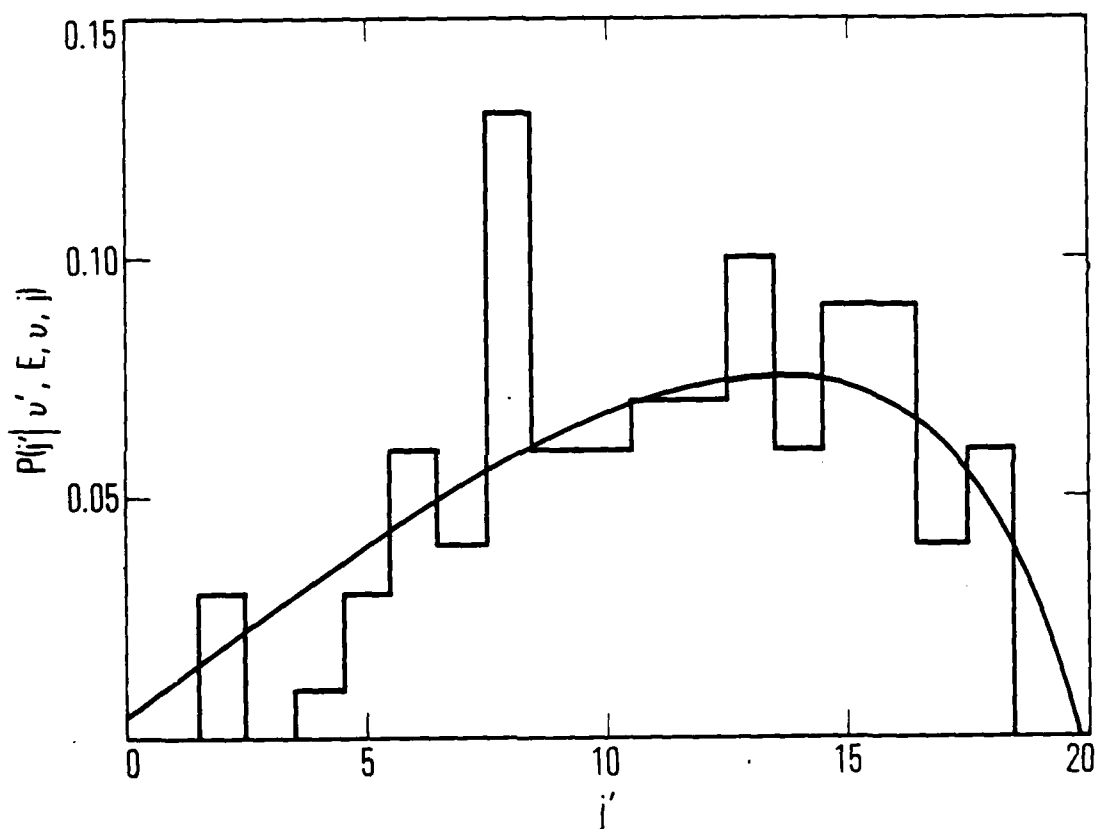


Figure 5. Product rotational distribution for the case $v = 1, j = 1, v' = 1$ and $E = 25$ k cal/mol. The histogram is the trajectory results computed using Eq. (13). The smooth curve is the analytic fit computed using Eq. (14) with the surprisal parameter $\theta = 0$. (The smooth curve was plotted for visual convenience; only the integer values of j' have physical meaning.)

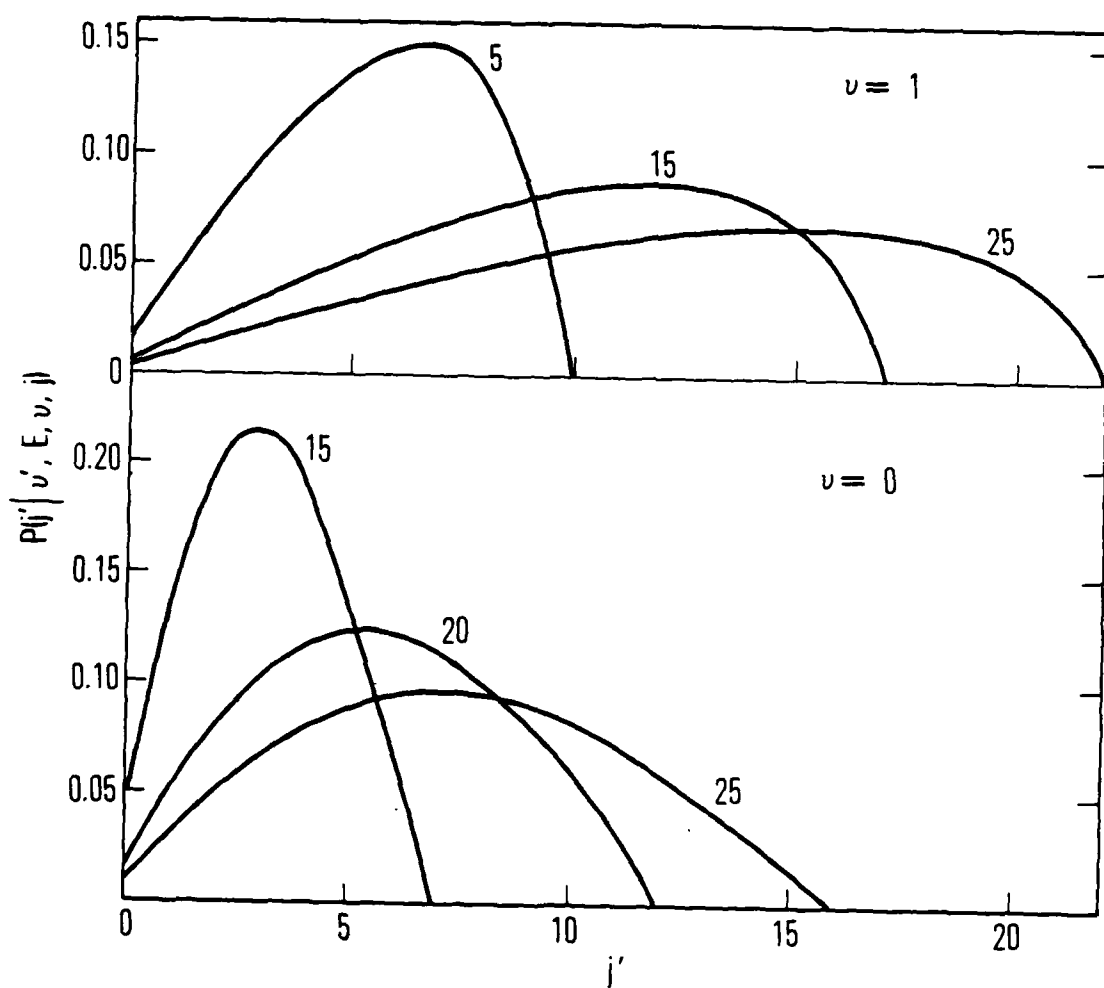


Figure 6. Product rotational distributions computed using the analytic fit Eqs. (14) - (21). Each curve is labeled with the initial relative kinetic energy E (kcal/mol) of the reactants; v is the initial vibrational state.

the vibrationally resolved cross section, given analytically by Eq. (9), by the rotational probability function, given analytically by Eq. (14), to obtain

$$\sigma_r(V, v, j; v', j') = P(j' | v'; V, v, j) \sigma_r(V, v, j; v') \quad (22)$$

This formula is the main result of this report. It represents (implicitly) the state-to-state cross sections as a product of three factors, each of which is a simple analytic (least squares fit) formula. The three factors are the reaction cross section given by Eq. (5), the vibrational probability distribution given by Eq. (7) and the rotational probability distribution given by Eq. (14). This analytic formula, along with the parameters given in Tables 2 and 3 and Eqs. (18) - (21), provides an efficient means for calculating the state-to-state reactive cross sections for the $O + H_2$ reaction.

REFERENCES

1. B. R. Johnson and N. W. Winter, "Classical trajectory study of the effect of vibrational energy on the reaction of molecular hydrogen with atomic oxygen," J. Chem. Phys. 66, 4116 (1977).
2. G. C. Light, "The effect of vibrational excitation on the reaction of $O(^3P)$ with H_2 and the distribution of vibrational energy in the product OH," J. Chem. Phys. 68, 2831 (1978).
3. D. E. Howard, A. D. McLean and W. A. Lester, "Extended basis first-order CI study of the $^1A'$, $^3A''$, and \tilde{B}^1A' potential energy surfaces of the $O(^3P, ^1D) + H_2(^1\Sigma_g^+)$ Reaction," J. Chem. Phys. 71, 2412 (1979).
4. S. P. Walch, T. H. Dunning, Jr., R. C. Raffanetti and F. W. Bobrowicz, "A theoretical study of the potential energy surface for $O(^3P) + H_2$," J. Chem. Phys. 72, 406 (1980).
5. R. S. Schinke and W. A. Lester, Jr., "Trajectory study of $O + H_2$ reactions on fitted ab initio surfaces. I. Triplet case," J. Phys. Chem. 70, 4893 (1979).
6. CLASTR was written by J. T. Muckermann and is available from the Quantum Chemistry Program Exchange. Additional details are given in: (a) J. T. Muckermann, J. Chem. Phys. 54, 1155 (1971); (b) ibid., 56, 2997 (1972) (c) ibid., 57, 3388 (1972).
7. M. Karplus, R. N. Porter and R. D. Sharma, "Exchange reactions with activation energy. I. Simple barrier potential for (H, H_2) ," J. Chem. Phys. 43, 3259 (1965).
8. G. H. Herzberg, Molecular Spectra and Molecular Structure. I. Spectra of Diatomic Molecules, Van Nostrand, New York (1950).
9. R. D. Levine, R. B. Bernstein, P. Kahana, I. Procaccia, and E. T. Upchurch, "Surprisal analysis and probability matrices for rotational energy transfer," J. Chem. Phys. 64, 796 (1976).
10. R. D. Levine and J. L. Kinsey, "Information: Theoretic Approach: Application to Molecular Collisions," in Atom-Molecule Collision Theory, R. B. Bernstein, editor, Plenum Press, New York (1979). Chapter 22.
11. R. D. Levine and R. B. Bernstein, "Thermodynamic Approach to Collision Processes," in Modern Theoretical Chemistry, Vol. 2, Part B, W. H. Miller, editor, Plenum Press, New York (1976). Chapter 7.

LABORATORY OPERATIONS

The Laboratory Operations of The Aerospace Corporation is conducting experimental and theoretical investigations necessary for the evaluation and application of scientific advances to new military space systems. Versatility and flexibility have been developed to a high degree by the laboratory personnel in dealing with the many problems encountered in the nation's rapidly developing space systems. Expertise in the latest scientific developments is vital to the accomplishment of tasks related to these problems. The laboratories that contribute to this research are:

Aerophysics Laboratory: Launch vehicle and reentry aerodynamics and heat transfer, propulsion chemistry and fluid mechanics, structural mechanics, flight dynamics; high-temperature thermomechanics, gas kinetics and radiation; research in environmental chemistry and contamination; cw and pulsed chemical laser development including chemical kinetics, spectroscopy, optical resonators and beam pointing, atmospheric propagation, laser effects and countermeasures.

Chemistry and Physics Laboratory: Atmospheric chemical reactions, atmospheric optics, light scattering, state-specific chemical reactions and radiation transport in rocket plumes, applied laser spectroscopy, laser chemistry, battery electrochemistry, space vacuum and radiation effects on materials, lubrication and surface phenomena, thermionic emission, photosensitive materials and detectors, atomic frequency standards, and bioenvironmental research and monitoring.

Electronics Research Laboratory: Microelectronics, GaAs low-noise and power devices, semiconductor lasers, electromagnetic and optical propagation phenomena, quantum electronics, laser communications, lidar, and electro-optics; communication sciences, applied electronics, semiconductor crystal and device physics, radiometric imaging; millimeter-wave and microwave technology.

Information Sciences Research Office: Program verification, program translation, performance-sensitive system design, distributed architectures for spaceborne computers, fault-tolerant computer systems, artificial intelligence, and microelectronics applications.

Materials Sciences Laboratory: Development of new materials: metal matrix composites, polymers, and new forms of carbon; component failure analysis and reliability; fracture mechanics and stress corrosion; evaluation of materials in space environment; materials performance in space transportation systems; analysis of systems vulnerability and survivability in enemy-induced environments.

Space Sciences Laboratory: Atmospheric and ionospheric physics, radiation from the atmosphere, density and composition of the upper atmosphere, aurorae and airglow; magnetospheric physics, cosmic rays, generation and propagation of plasma waves in the magnetosphere; solar physics, infrared astronomy; the effects of nuclear explosions, magnetic storms, and solar activity on the earth's atmosphere, ionosphere, and magnetosphere; the effects of optical, electromagnetic, and particulate radiations in space on space systems.

DATE
FILMED
-8